Open loop optical performances of a 277 voice coil actuators deformable mirror.

Runa Briguglio[a], Chiara Selmi[b], Lorenzo Busoni[a], Guido Agapito[a], Marco Bonaglia[a], and Paolo Grani[a]

[a]INAF Osservatorio Astrofisico Arcetri L. E. Fermi 5, 50125 Firenze Italy

ABSTRACT

We report the optical calibration and open loop qualification of an ALPAO-DM277 deformable mirror in the laboratory. The device is part of the test equipment for ERIS, the ESO second generation adaptive optics module, as the simulator of the VLT-UT4 adaptive secondary. The laboratory characterization includes the measurement of the actuator influence functions, the flattening command, the measurement of the long-term optical stability and repeatability of the command applied, the measurement of the fitting error of the KL command matrix. The findings are also discussed in the frame of future AO systems, where such DMs might be exploited as open loop correctors in front of the WFS.

Keywords: Adaptive Optics, Wavefront correctors, Deformable mirrors, Optical calibration, Laser Interferometry

1. THE ERIS AO TEST-BED WITH THE ALPAO DM

ERIS-AO[1,2] is the second generation AO[3] instruments for the VLT-UT4; it will be installed in Paranal in 2020 and after commissioning will deliver a corrected wavefront to the instruments NIX (imager) and SPIFFIER, an updated version of the SPIFFI spectrograph. The system is currently (June 2019) under integration at INAF-Osservatorio Astrofisico di Arcetri and will undergo a test campaign before the Acceptance in Europe. In order to perform the close loop test and performance verification, a dedicated test-bed has been integrated to simulate the UT-4 telescope with its adaptive secondary mirror (DSM).[4] The DSM simulator is composed by two fiber sources, for both NGS and LGS, and an optical system to reproduce the F/13.6 beam from the VLT Cassegrain. The DSM is simulated by a 277 actuator ALPAO-DM, which defines also the system stop. The optical diameter is 21.7 mm (vs a 25 mm clear aperture of the mirror) so that in the end the total number of actuators to be used in the AO loop is 222 or lower, depending on the illumination threshold set on the Shack-Hartmann WFS.
The ALPAO-DM has been characterized in laboratory before integration on the test-bed, in order to measure the influence functions (IF) of the visible actuators and calibrate the best flattening command on the optical area and to compute the KL modal basis for the AO loop. Additionally, we performed a number of test to characterize the DM for open loop operations. In facts, there is an increasing interest in open loop or pseudo-open loop correction strategies for the next generation AO systems (e.g. MAORY[9]). The literature[5,6,7] reports thermal drifts and memory effects encountered on this commercial DMs, so our additional verification is intended as a test-bench for implementation in future AO projects.

2. OPTICAL CALIBRATION

2.1 Test bed and procedure

The DM has been installed on a dedicated optical table in front of a 4D-Technology Twyman-Green dynamic interferometer. The 4D has an output beam of 8 mm so that we assembled a custom beam expander with laboratory lenses to produce a suitable measuring beam. The DM surface is focused on the 4D camera thanks to the lenses assembly. Air convection within the beam is considered negligible (since the beam itself is 25 mm wide

Further author information:
Runa Briguglio: E-mail: runa@arcetri.astro.it, Telephone: +39 055 2752200

only) and the mechanical vibrations are controlled thanks to the air-insulation provided by the optical table. A comprehensive and general description of the calibration procedure for DMs is given in.[8] Here we recall quickly that the first step is the optical alignment in front of the interferometer, by adjusting the beam expander to null the first order Zernike terms, namely focus, coma, astigmatism and spherical aberrations. In order to prevent the alignment print-through on the DM, the optical alignment is performed on a reference flat mirror, placed at the DM location: the final alignment residual is 10 nm RMS WF. Conversely, tip/tilt is adjusted on the DM itself, which is mounted on a commercial pitch/yaw platform.
The core of the optical calibration is based on the measurement of the actuator influence functions, i.e. the collection of the WF signal corresponding to the application of a unitary command to all the actuators. Such data are piled up into the optical interaction matrix M, representing therefore a link between the interferometer measurements and the actuators commands.

2.2 Mirror flattening

The flattening[8] consists in the nulling of the WF, as seen by the interferometer, within the DM correction space. Let be w_i be the current wavefront map, the corresponding flattening command c_i is computed as $c_i = -Rw_i = M^+w_i$, where R is the system reconstruction matrix. Since the command is applied with negative amplitude, the effect is to null the WF features matching the actuators influence functions.
The starting condition is with the DM just powered-up, without any factory-calibrated command; the WFE is 485 nm RMS (as shown in Fig.1), due to mostly power and astigmatism. After flattening the WFE is 5 nm RMS (see Fig. 2). As experienced during former DM calibration activities, the flattening command is applied with gain equal to 1, i.e. the procedure is expected to converge in a single step. Such behaviour was observed (within measurement noise) also on this commercial DM.

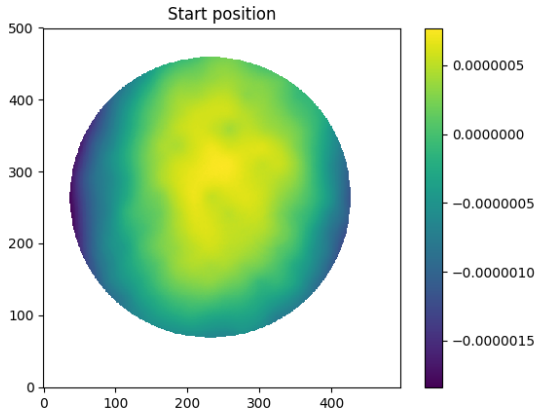

Figure 1. Surface map of the DM after power-up, with no command applied, i.e. all actuators are in rest position with zero command.

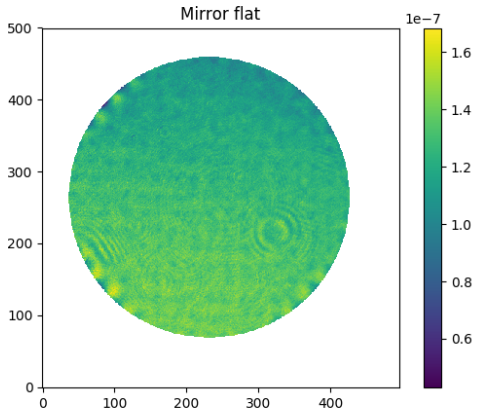

Figure 2. Surface map of the DM after applying the flattening command in close loop with the interferometer.

2.3 Fitting of Zernike and KL modes

The interaction matrix M was used to produce Zernike shapes and to test the fitting of Kahrunen-Loewe modes with the DM. Both basis are necessary to first align the DM and the ERIS WFS and then successfully close the AO loop: hence the optical pupil should be reduced to a 21.7 mm diameter as for the DSM simulator design. Since a number of actuators lay outside the optically controlled area, we excluded them by masking the influence functions accordingly and then filtering the SVD of the M matrix. Once this new reconstructor was obtained, we computed the mirror commands to produce the wanted Zernike modes (1 to 11, following the Noll numbering) and the first 222 KL modes. As a verification we measured these basis with the same procedure as for the influence functions. Then we evaluated the fitting error by computing the RMS of the difference between the theoretical shape and the measured one. In Fig. 3 and 4 we present the results in terms of fractional fitting error.

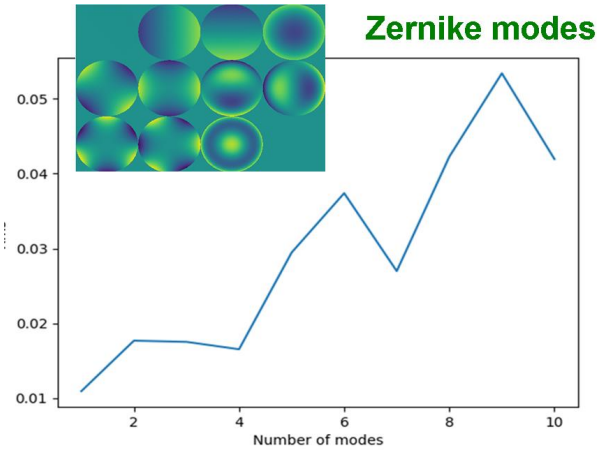

Figure 3. Fitting error (as fraction of the command amplitude applied) of the first Zernike modes and the surface maps obtained.

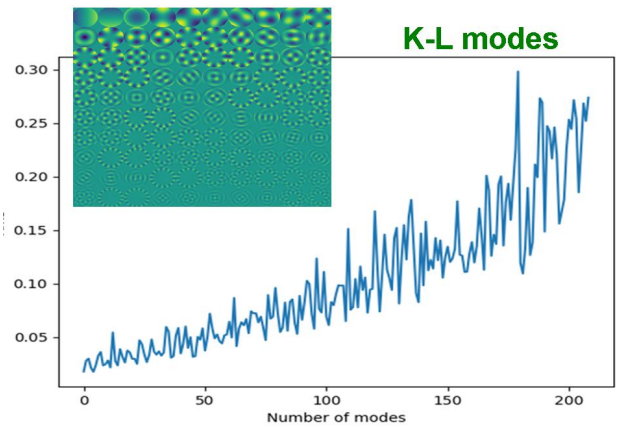

Figure 4. Fitting error (as fraction of the command amplitude applied) of the KL modes fitted and the surface maps obtained.

3. CHARACTERIZATION OF OPEN LOOP BEHAVIOUR

We investigated the open loop performances of the DM since we noticed drifts after applying the flattening command; such drifts turned out to be connected with the last shape assumed (and maintained) by the mirror, thus triggering the suspect that the phenomenon could be related to creep or material memory in general. We found that similar effects are also reported in the literature. We also noticed a drift occurring after the DM is exercised with a command history. In the following sections we summarize the test procedures and the findings.

3.1 Memory effect

We observed that immediately after flattening, the DM tends to assume a shape that is a combination of focus and astigmatism. Such shape is very similar to the membrane rest shape, i.e. the shape assumed by the optical surface when no command is applied to the actuators. Such effect has an exponential decay law, whose amplitude tends to saturate after a sequence of consecutive corrections. Which means that the observed amplitude is lower and lower when the drift is corrected in close loop. The fact that the drifting shape is observed after the first flattening and corresponds to the rest shape (i.e. the last shape assumed by the DM) suggested the idea that the drift is related to a memory effect. We then investigated the temporal, amplitude and spatial frequency response of such effect.
The test consists in the application of KL modes with a given amplitude a and for a given time duration τ; then the command is removed and the mirror is monitored continuously with the interferometer. We selected KL modes since they allows testing in different spatial scale regimes. The test procedure is summarized as follows:

1. after power-up, we continuously flat the mirror by running iteratively the flattening procedure, with a time cadence of a few minutes for an hour; in this way, we get rid of the *first shape* memory effect;
2. we apply the KL mode i with amplitude a_j and keep it on the DM for a time τ_k;
3. after the time lag τ_k the command is released i.e. the last flattening command is applied with no interferometer feedback;
4. the DM is monitored at a given cadence (a few seconds) with the interferometer producing a phase map $\omega_{i,j,k,x}$, where the subscript x indicates the frame sequence;
5. each frame is matrix multiplied with the inverse matrix of the KL interaction matrix, obtaining a vector of coefficients representing the modal content of the phase map $\omega_{i,j,k,x}$.

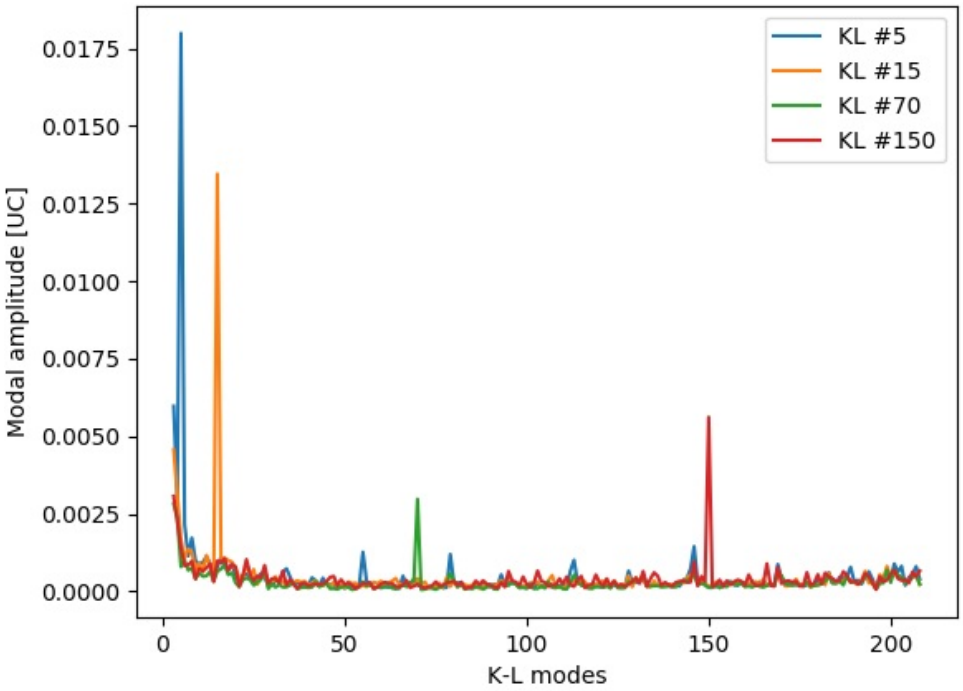

Figure 5. Modal content of the DM WF after (minutes) relaxing the static shape applied. The different colors indicate the test with different KL modes applied as static shape. The plots indicates that within noise the WF deformation due to memory effect matches very well with the static shape applied.

The procedure is iterated for all the selected KL modes, the amplitudes a and the time durations τ and in the end we obtain the mirror modal coefficientes during the *discharging* phase.
In Fig.5 we show the modal coefficients of a phase maps taken some minutes after relaxing the static shape, for each sequence: we observe that the shapes excited matches with the KL applied (within noise), which means that the memory effect is command dependant. The label *UC* in the vertical axis is for *unit command*, which is the maximum applicable command amplitude (± 1). In Fig.6 we show the modal coefficient corresponding to the excited KL command during the test time gap (we plotted a single amplitude and excitation time only).

3.2 Thermal drift

We noticed a WFE degradation when the system is excited with the application of large amplitude commands. This was observed after opening the optical loop correcting a disturbance time history: the loop quality, conversely, was very stable. We guessed that the membrane reacts to command excitation by introducing an drifting shape that matches well with the actuator influence functions, so that the optical loop is able to recover it with very good fitting error.
To assess this effect we designed and carried out a dedicate laboratory test, according the procedure describe below:

1. the mirror is powered up and flattened; the flattening is iterated several times for (e.g.) an hour to get rid of the rest shape memory effect (as discussed in the previous section).
2. an actuator commands sequence is created: each frame has a random pattern over the actuators and the amplitude is adjusted to have maximum (minimum) value equal to 1 (-1);
3. each frame is scaled to have a standard deviation equal to σ_i; the σ values are chose to reduce the command amplitude and preserve the unitary peak and valley values;

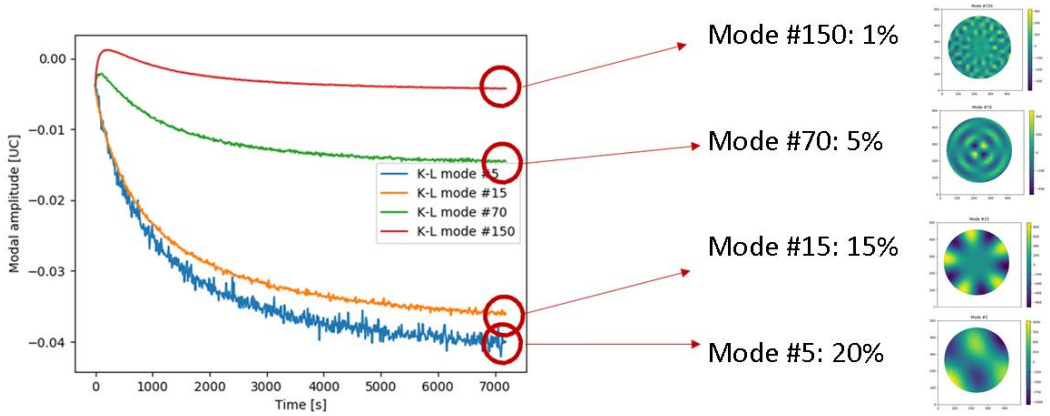

Figure 6. Measured modal amplitude due to memory effect, for the 4 modes tested, during the relaxation period. The asymptotic amplitude depends on the modal spatial scale.

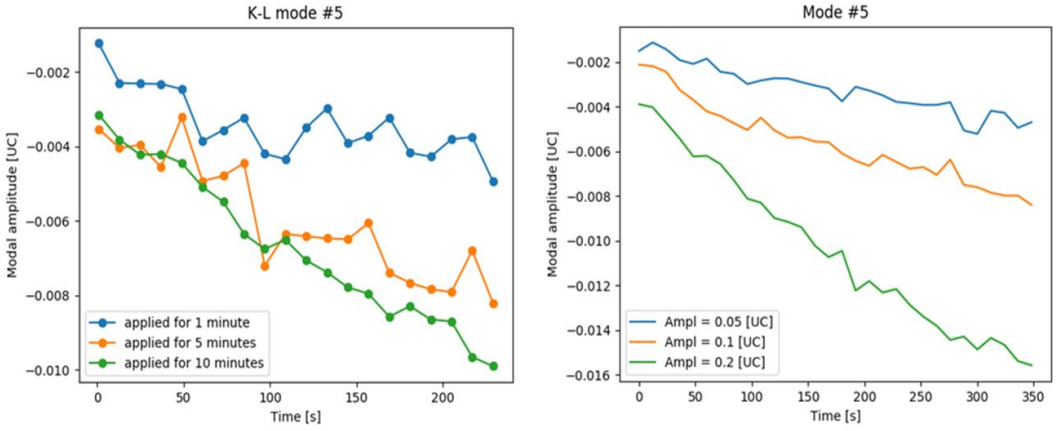

Figure 7. Left: measured modal amplitude due to memory effect for mode #5 after being applied on the DM for 1, 5 and 10 minutes. Right: same plot, with different initial amplitude of the mode.

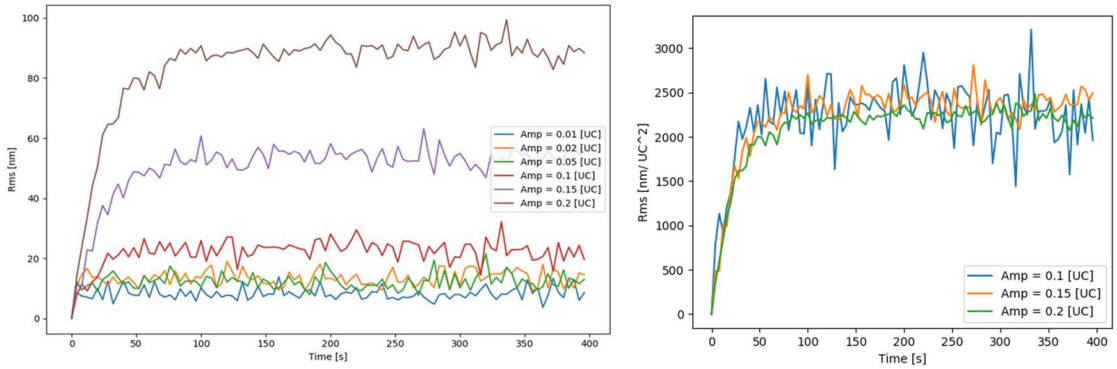

Figure 8. Left: surface RMS of the DM as a function of time, after the end of the command sequence, as a consequence of the thermal drift. Right, same plot, after normalizing with the square of the command amplitude applied.

4. the time history is applied at 25 Hz frequency, with not optical feedback;
5. after the sequence is completed, the last flattening command is loaded;
6. the mirror is monitored with the interferometer at a cadence of 1 s, for a time duration of 10 minutes.

After collecting the dataset, we analyzed the frames captured during the last step of the procedure to compute the WFE difference with respect to the first frame in the sequence. The result is shown in Fig.8, left panel, for the various amplitudes of the command sequence applied. For very low command amplitudes the WFE variation is not distinguished from measurement noise, while for larger command amplitudes we observed a steep variation of the WFE that reaches its maximum after approximately 1 minute after stopping the command sequence. The amount of variation is proportional with the amplitude of the command sequence. In the right panel, we normalized the WFE variation to the square value of the command amplitude; we observe that the plots are sumperimposed. Since the command amplitude is linearly proportional to the current through the actuators, the square of the amplitude corresponds to the power dissipated. We observe therefore that the WFE variation is linearly dependent from the thermal dissipation within the system. The shape corresponding to such deformation is composed by a mix of power and astigmatism, resembling the same shape when the system is off (i.e. no command aplied).

4. CONCLUSION

We installed and tested with the interferometer an ALPAO DM 277 deformable mirror, controlled with voice coil actuators over a 25 mm diameter optical area. The DM is used as a simulator of the VLT UT-4 DSM during the calibration and acceptance test of the ERIS WFS. The DM was flattened in a single step delivering a 5 nm RMS surface error after correcting 277 modes. We fitted both Zernike modes (tilt to spherical aberrations, resulting in a maximum fitting error for Z9 of 5%) and KL modes created over a smaller optical area, to match the stop size in the ERIS test-bed. The KL are requested for the close loop tests with the ERIS WFS, so that we created 222 modes but we consider for use just 150 approximately.
The qualification of the DM included (beyond the standard recipe) the verification of its performances for open loop operations, in order to evaluate its possible implementation for the next generation WFS such as MAORY for the ELT. We reported a memory effect, consisting in a DM WFE corresponding to the last static shape applied and maintained over a given period (minutes). We also reported a WF drift observed after the DM was exercised with a command history with given amplitude. The drift amplitude is proportional with the command history one. Both phenomena were already reported in the literature and shall be considered a major show-stopper for open-loop operations. On the contrary, the close loop performances are as expected and globally very good.

REFERENCES

[1] Riccardi, A., Esposito, S., Agapito, G. & al.: *"The ERIS adaptive optics system"*, Proc. SPIE 9909, Adaptive Optics Systems V, 99091B (26 July 2016).

[2] Riccardi, A., Esposito, S., Agapito, G. & al.: *"The ERIS adaptive optics system: from design to hardware"*, Proc. of SPIE, Vol 10703, 2018

[3] Davies, R., Esposito, S., Schmid, H. -M., & al.: *ERIS: revitalising an adaptive optics instrument for the VLT* Proc. of SPIE, Vol 10702, 2018

[4] Briguglio, R., Biasi, R., Xompero, M., & al: *"The deformable secondary mirror of VLT: final electro-mechanical and optical acceptance test results"*, Proc. SPIE 9148, Adaptive Optics Systems IV, 914826 (21 July 2014).

[5] Bitenc, U.: *"Software compensation method for achieving high stability of Alpao deformable mirrors"*, Opt. Express, Vol. 25, No. 4, (February 2017).

[6] Bitenc, U., Bharmal, N.A., Morris, T.J.and Myers, R.M.: *"Assessing the stability of an ALPAO deformable mirror for feed-forward operation"*, Opt. Express, Vol. 22, No. 10, (May 2014).

[7] Le Bouquin, J.B., Berger, J.P., Beuzit, J.L & al.: *"Characterization of ALPAO deformable mirrors for the NAOMI VLTI Auxiliary Telescopes adaptive optics"*, Proc. Society of Photo-Optical Instrumentation Engineers (SPIE), Vol. 10703, Adaptive Optics Systems VI, (July 2018).

[8] Briguglio R., , Quirs-Pacheco, F.: , Males, J. R., & al: *"Optical calibration and performance of the adaptive secondary mirror at the Magellan telescope"*, Scientific Reports, Volume 8, (July 2018).

[9] E. Diolaiti, P. Ciliegi, R. Abicca, & al.: *"MAORY: adaptive optics module for the E-ELT"*, Proc. SPIE 9909, Adaptive Optics Systems V, 99092D (27 July 2016).